CellPress
OPEN ACCESS

Trends in
Cancer

Review

Crosstalk of T cells within the ovarian cancer microenvironment

Bovannak S. Chap[1,2,3], Nicolas Rayroux[1,2,3], Alizée J. Grimm[1,2,3], Eleonora Ghisoni[1,2,3], and Denarda Dangaj Laniti[1,2,3,*]

Ovarian cancer (OC) represents ecosystems of highly diverse tumor microenvironments (TMEs). The presence of tumor-infiltrating lymphocytes (TILs) is linked to enhanced immune responses and long-term survival. In this review we present emerging evidence suggesting that cellular crosstalk tightly regulates the distribution of TILs within the TME, underscoring the need to better understand key cellular networks that promote or impede T cell infiltration in OC. We also capture the emergent methodologies and computational techniques that enable the dissection of cell–cell crosstalk. Finally, we present innovative *ex vivo* TME models that can be leveraged to map and perturb cellular communications to enhance T cell infiltration and immune reactivity.

Highlights

The immune status of the ovarian cancer (OC) tumor microenvironment (TME) can be systematically classified based on CD8$^+$ T cell densities and spatial distribution within tumor and stromal regions.

OC immunophenotype classification captures distinct immune cell networks which regulate T cell infiltration and antitumor immunity both at diagnosis and upon treatment or disease evolution.

Cellular networks can be employed as tissue biomarkers to improve patient selection for therapy and reveal new targetable pathways which can disrupt the strong immunosuppression and exclusion prevalent in OC.

Integration of advanced computational and imaging approaches can unravel the spatiotemporal TME heterogeneity of OC.

Modeling and perturbation of cellular crosstalk via *ex vivo* 3D tumor model systems can further dissect key cellular crosstalk across OC immune phenotypes and identify new therapeutic targets.

The concept of CD8$^+$ T cell-based tissue immune phenotype and its association with prognosis in ovarian cancer

Over the past few years, immunotherapy has transformed the treatment landscape for numerous solid tumors including a subset of gynecological cancers [1,2]. However, **immune checkpoint blockade** (**ICB**; see Glossary) has so far shown limited efficacy in high-grade serous ovarian cancer (HGSOC) (the most common histological subtype of epithelial ovarian cancer) [3,4], despite the immunogenic nature of this cancer type where half of patients showcase CD8$^+$ T cells within tumor beds at diagnosis [5–7]. Several factors, including low tumor mutational burden (TMB), increased aneuploidy, elevated copy-number alterations, and significant intratumoral heterogeneity (ITH) [8] could contribute to the lack of response to ICB [3,9]. Notably, most trials testing ICB in patients with OC performed thus far have involved unselected patient populations without upfront implementation of biomarkers.

Although CD8$^+$ T cells have been the subject of extensive investigation, accumulating research has drawn attention to the involvement of various other immune cell populations in shaping the TME and regulating antitumor immune responses in OC [3,10–12]. Given the emergence of immunotherapies and evidence of a central role of the immune system in sculpting and controlling tumor growth, elucidating the immune contexture of cancers has become an area of intense interest [13].

The Ovarian Tumor Tissue Analysis (OTTA) Consortium showed that HGSOC is the most T cell-infiltrated histotype, and CD8$^+$ intraepithelial tumor-infiltrating lymphocytes (ieTILs) are a favorable prognostic factor regardless of the extent of surgical cytoreduction, chemotherapy treatments, or an underlying germline *BRCA1* mutation [14]. Shedding light on some potentially predictive and prognostic biomarkers, it was recently shown that long-term HGSOC survivors tend to have several co-occurring alterations in genes associated with DNA repair and more frequent somatic variants than short-term or moderate-term survivors, resulting in an increased predicted neoantigen load and enhanced immune responses [15].

[1]Department of Oncology, Lausanne University Hospital, University of Lausanne, Lausanne, Switzerland
[2]Ludwig Institute for Cancer Research, Lausanne Branch, University of Lausanne (UNIL), Lausanne, Switzerland
[3]Agora Cancer Research Center, Lausanne, Switzerland

*Correspondence:
Denarda.Dangaj@chuv.ch (D. Dangaj Laniti).

Based on CD8$^+$ T cell infiltration patterns, OCs have been classified into so-called 'T cell inflamed' (also termed 'hot') tumors, in which T cells infiltrate both tumor deposits (islets) as well as the tumor-associated stroma, 'excluded' tumors, in which T cells sequester in the stroma but are absent from tumor islets, and 'non-inflamed' tumors (also called 'immune-desert' or 'cold' tumors) [3,11,16,17] (Figure 1, Key figure). Although this three-tier immune classification is generally accepted, it overlooks the commonly observed intratumoral heterogeneity of OC TME [11,18,19] and still lacks standardization. To bridge this gap, attempts have been made to employ integrated digital pathology approaches to standardize TIL measurements in OC tissues [16,20]. A machine learning-based classifier was able to capture the heterogeneity of CD8$^+$ T cell densities and their spatial distribution in whole tumor tissue slides imaged by multiplex immunofluorescence (mIF) [20]. This tumor immune classifier captures the continuum of CD8$^+$ T cell infiltration and defines four distinct OC **immune phenotypes**: homogenously or heterogeneously inflamed, excluded or desert OC tissues. These four immune phenotypes were associated with different clinical outcome and **homologous repair deficiency (HRD)** status. Importantly, they were characterized by differential TIL states and TME networks [20], suggesting that tumor immunophenotype classification can capture underlying distinct immune cell networks [11].

In this review we propose that these networks can (i) be employed as tissue biomarkers to improve patient selection and therapy in OC, and (ii) reveal new targetable pathways which can disrupt the strong immunosuppression that is prevalent in OCs.

Cellular networks orchestrating immune response in OC

Categorizing tumors by looking at the spatial distribution of CD8$^+$ T cells in the TME has permitted the investigation of infiltration, immune-exclusion, and desertification mechanisms [11,16] (Figure 1). It also provided a unifying framework to understand in-depth the underlying and distinct immune cell networks [11]. In the following we present cell–cell crosstalk that governs immune response and T cell infiltration in epithelial OC, with a focus on HGSOC.

Cell–cell networks in the inflamed TME of OC

Tumors with increased DNA damage (i.e., cells with HRD) can be constitutively inflamed. Accumulation of damaged DNA in the cytoplasm and subsequent cell-autonomous activation of the nucleic acid-sensing and type I interferon (IFN) pathways through cyclic GMP-AMP synthase–stimulator of interferon genes (cGAS-STING) [21,22] leads to upregulation of the JAK/STAT and tumor necrosis factor (TNF) pathway downstream genes and the secretion of **chemokines**, such as CCL5 and CXCL16, that attract T cells in tumor islets [11,23]. Patrolling tissue-resident T cells that recognize tumor antigens produce IFN-γ and polarize adjacent myeloid dendritic cells (DCs) and macrophages to secrete CXCL9/10 chemokines and attract CCR5$^+$, CXCR3$^+$, and CXCR6$^+$CD8$^+$ T cells to inflamed tissues [10]. Tumor-specific CD8$^+$ TILs may simultaneously engage tumor cell targets and co-stimulatory myeloid antigen-presenting cells (APCs). Tumor-specific expression of CCL5 in conjunction with CXCL9 promotes lymphocyte infiltration [23], and silencing of CCL5 expression leads to an attenuated immune response [22].

CXCR6 together with CD103 and CD69 expression on CD8$^+$ T cells indicate the differentiation of circulating T cells into tissue-resident T cells [24]. Following homing to the tumor, the persistence and sustained antitumor effector function of T cells is dependent on the balance between co-stimulatory and co-inhibitory interactions. In OC, the presence of mature DCs has been associated with improved prognosis [25]. Resident myeloid APCs support antitumor CD8$^+$ TILs by preventing terminal **T cell exhaustion** and maintaining stem-like T cells niches through direct CD80/CD86–CD28 co-stimulation [12] and paracrine support by interleukin (IL)-12 and IL-15 cytokines. Pre-existing myeloid

Glossary

Adoptive cell transfer (ACT): a treatment in which T cells are collected from a patient, modified or expanded *in vitro*, and then reinfused to the patient to attack tumor cells. ACT has shown beneficial outcomes in melanoma patients.
Chemokines: small proteins that attract immune cells expressing specific binding receptors. Chemokines are distinguished by cysteine residues: in CCL chemokines the two cysteines are adjacent, whereas in CXCL chemokines they are separated by one amino acid.
Extracellular matrix (ECM): the complex network of extracellular macromolecules, such as collagen, enzymes, and glycoproteins, that surround cells and provide structural and biochemical support.
Ferroptosis: cell death initiated through iron-dependent lipid peroxidation.
Homologous repair deficiency (HRD): a phenotype present in half of ovarian cancer (OC) cases, which is defined as an inability to repair double-strand breaks in DNA via the homologous recombination (HR) pathway, thus inducing immunogenicity.
Immune checkpoint blockade (ICB): monoclonal antibodies that are used to treat cancer by disrupting the interaction of checkpoint proteins with their ligands (i.e., PD-1, PD-L1, CTLA-4).
Immune phenotype: a classification system focusing on the localization, distribution, and abundance of CD8$^+$ T cells within the TME that categorizes tumors as inflamed, excluded, or deserts by histopathological assessment.
T cell exhaustion: describes T cells that exhibit reduced effector function (i.e., granzyme B, perforin, IFN-γ, TNF-α), decreased proliferative capacity, and increased expression of co-inhibitory receptors (i.e., PD-1, CTLA-4, TIM-3, LAG-3)
Tertiary lymphoid structure (TLSs): organized lymphoid aggregates that form in non-lymphoid organs during chronic inflammation and are associated with a local adaptive immune response.

Key figure

A systematic multi-omic workflow to decipher cellular crosstalk in ovarian cancer (OC)

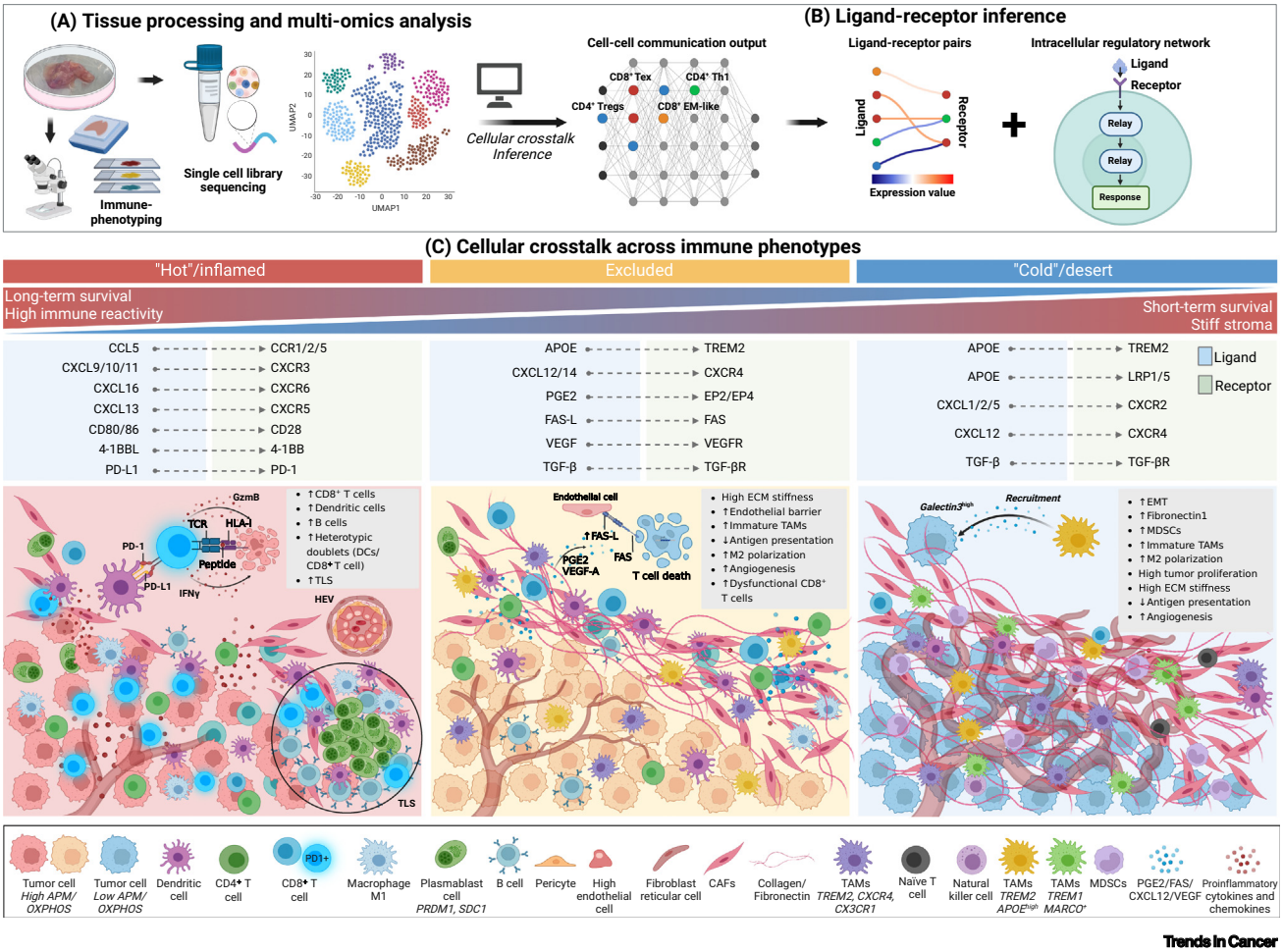

Figure 1. (A) Resected tumors undergo histopathological evaluation and subsequent multiplex immunofluorescence (mIF) imaging analysis to define CD8$^+$ T cell-based immune categorization; tumors are classified into 'hot'/inflamed, excluded, or 'cold'/desert tumors. Next, single-cell analysis is used to infer the main immune cell subtypes and cellular networks. (B) Computational analysis through inferred ligand–receptor pairs and intracellular regulatory networks reveal key cellular interactions among the different immunophenotypes. (C) (Top) Main ligand–receptor interactions across tumor immune phenotypes. (Bottom) Schematic cartoon representation of the major cellular components and crosstalk involved in each immune phenotype. (Inflamed) Characterized by high immune reactivity and cellular crosstalk including chemokine–chemokine receptor interactions, antigen recognition, co-stimulation, and co-inhibition. This phenotype exhibits a high presence of intraepithelial CD8$^+$ T cells, mature myeloid cells such as dendritic cells and B cells, and tertiary lymphoid structures (TLSs). (Excluded) Dominated by prostaglandin E2 (PGE2), FAS ligand (FAS-L), vascular endothelial growth factor (VEGF), and transforming growth factor (TGF)-β signaling, this immune phenotype excludes antigen-experienced T cells from the tumor beds. (Desert) Characterized by lack of antigen presentation and immune interactions. Cancer-associated fibroblasts (CAFs) and reactive stroma increase the stiffness of the extracellular matrix (ECM) to recruit or retain immunosuppressive cells such as myeloid-derived suppressor cells (MDSCs) and tumor-associated macrophages (TAMs), resulting in immune evasion and tumor progression. Abbreviations: APM, antigen-processing machinery; 4-1BB (CD137), tumor necrosis factor receptor superfamily member 9; CCR, C-C chemokine receptor; CXCL, C-X-C motif chemokine ligand; CXCR, C-X-C motif chemokine receptor; DCs, dendritic cells; EM, effector memory cell; EMT, epithelial-to-mesenchymal transition; GzmB, granzyme B; HEV, high endothelial venule; OXPHOS, oxidative phosphorylation; TCR, T cell receptor; Tex, exhausted T cell; Th1, type 1 T helper cell; Treg, regulatory T cell; UMAP, uniform manifold approximation and projection. Figure generated with BioRender.

APC and APC:TIL niches are crucial for effective PD-1 blockade [12,26] and also for the response to adoptive T cell therapy [27].

Besides the aforementioned TIL myeloid crosstalk, several studies have shed light on the crucial role of B cell responses in antitumor T cell immunity and inflammation [28]. Inflamed OCs are enriched in proliferating plasmablasts with overexpression of *PRDM1*, *SDC1*, and *CD38* [10], whereas the detection of plasma cells in **tertiary lymphoid structures (TLSs)** indicates increased cytolytic features of TILs [29]. Interestingly, TILs were associated with improved survival only when co-present with $CD138^+$ intratumoral plasma cells that displayed a dominant IgA switch redirecting myeloid cells and sensitizing OC cells to T cell-mediated cytolysis [30]. Patient-derived OC cells are also frequently coated with IgGs, and tumor-reactive autoantibodies can occur naturally or evolve through an antigen-driven selection process via somatic hypermutation [31]. In addition, tumor-infiltrating B cells might provide costimulatory signals to tumor-resident CXCL13-secreting TILs. The CXCL13-CXCR5 axis is essential for the early phase of TLS formation in OCs [32]. Intriguingly, OC TLS were associated with increased intratumoral density of more terminally differentiated $TIM3^+PD1^+CD8^+$ T cells [29], in contrast to lung cancer where TLSs are enriched in stem-like $TCF1^+PD1^+CD8^+$ T cells. More research will be necessary to unveil the cell–cell crosstalk and molecular networks which regulate TLS neogenesis and establishment in OCs. Syngeneic preclinical models that can give rise to TLSs will prove crucial to dissect the cell–cell crosstalk occurring between TLS and the OC TME (see Outstanding questions). In summary, the simultaneous presence of $CD8^+$ TILs, mature myeloid cells, B cells, and TLSs are linked to a favorable clinical OC prognosis [33].

Cell–cell networks in the excluded and desert TME of OC

In contrast to inflamed immune phenotypes, excluded and desert OCs exhibit low infiltration of $CD8^+$ T cells within the intraepithelial tumor compartment and therefore low immune reactivity. In excluded tumors, TILs are restrained in the stromal area, possibly owing to a mechanophysical barrier which involves the tumor endothelial vasculature, the fibrotic matrix deposited by cancer-associated fibroblasts (CAFs), and also M2-like macrophages characterized by *TREM2/CD169/CXCR4/CX3CR1* expression [11].

Upon recruitment, T cell homing to the tumor relies on the presence of a permissive endothelium. Secretion of proinflammatory cytokines promotes endothelial activation, leading to the creation of patches of activated endothelial cells expressing cell-adhesion molecules (selectins, ICAM-1, VCAM-1, etc.) that are required for endothelial–T cell adhesion and T cell extravasation. In excluded tumors, T cell recruitment can be hindered due to downregulation and/or declustering of adhesion molecules, or via secretion of endothelin β or vascular endothelial growth factor A (VEGF-A) and prostaglandin E2 (PGE2) that cooperatively induce FAS ligand (FASL) expression on endothelial cells, mediating selective apoptosis of effector T cells while leaving regulatory T cells (Tregs) unaffected [34]. The PGE2-EP2/EP4 axis, reinforced by genotoxic therapy [20], suppresses T cell-mediated anticancer immunity by inducing **ferroptosis** in antigen-experienced exhausted TILs [35] and preventing their effector differentiation [36] in the TME. In addition, the VEGF/VEGFR axis adversely impacts on APCs and effector T cells and enhances infiltration of Tregs and myeloid-derived suppressor cells (MDSCs) [37]. It is tempting to speculate that the stroma of excluded tumors selectively kills tumor-reactive but exhausted TILs through mechanisms such as FAS/FASL and PGE2-EP2/EP4, and allows the retention and expansion of more naïve/central memory TIL compartment.

Considering the major role of the **extracellular matrix (ECM)** in immune responses, efforts have been made to deconstruct and subsequently reconstruct the stroma features of omental metastatic deposits, a frequent niche of OC tumor invasion. A multilevel analysis of OC metastases revealed matrix index (matrisome) changes that were shared across solid tumors and could predict

the survival of patients with OC. It also uncovered a significant relationship between tissue stiffness conferred by upregulation of collagen-remodeling genes (*COL11A1*, *COMP*, *VCAN*, *FN1*, *COL1A1*, and *CTSB*) and disease progression [38] that is probably driven by transforming growth factor β (TGF-β) signaling [39].

CAFs are central for ECM remodeling. They can form a physical barrier to $CD8^+$ T cell infiltration by modulating the ECM of the TME via the production of cytokines (i.e., IL-6, TNF), growth factors (i.e., TGF-β, VEGF), chemokines (i.e., IL-1, IL-6, CXCL1, 2, 5, and 12, and CCL2 and 3), and matrix-remodeling enzymes [matrix metalloproteinases (MMPs)] [40–42]. Recently, two fibroblast subsets have been identified, one marking normal stroma and the other marking desmoplasia (i.e., a neoplasia-associated alteration in fibroblasts and ECM with distinct tissue morphology). Desmoplastic fibroblasts not only overexpress collagen fibril organization and ECM genes but also upregulate CXCL12 (the cognate ligand of CXCR4) and are associated with niches enriched in naïve T/natural killer (NK) cells [43]. It is still not clear whether ECM and CAFs actively exclude tumor-reactive TILs from entering the tumor beds or simply retain them in more naïve states.

Likely due to dysfunctional myelopoiesis mechanisms, OCs actively recruit immature myeloid cells and alternatively activated (M2-polarized) macrophages. APCs isolated from patients with OC appear to have functional deficiencies [35], with low CD80 and CD86 expression and diminished production of IL-12. They upregulate immune checkpoint ligands, suppressive cytokines, TGF-β, VEGF-A, and enzymes such as arginase and indoleamine 2,3-dioxygenase 1 (IDO1) that deplete key amino acids from the TME [44]. These immunosuppressive myeloid cells accumulate intracellular reactive oxygen species that provoke endoplasmic reticulum stress and increased lipid peroxidation [45], and promote upregulation of PGE2 [46].

While TIL-excluded tumors are dominated by *TREM2*-overexpressing $CD169^+$ macrophages characterized by tumor-associated macrophage (TAM)-like signatures, immune-desert tumors are infiltrated by $TREM1^+FCN1^+$ monocytes and $MARCO^+$ macrophages with MDSC-like signatures [11], indicating that specialized immune networks underlie distinct OC phenotypes. Recent findings highlight increased cell–cell crosstalk between macrophages and DCs in excluded and desert OC [20]. These networks establish complex cell interactions that secure immune tolerance. Finally, little is known about the involvement of $CD4^+$ T cells or of the role of other innate cells such as innate lymphoid cells, neutrophils, and mast cells for the tumor desertification process [3].

In summary, excluded tumors are characterized by low infiltration of activated $CD8^+$ T cells into the intraepithelial compartment and an increased presence of naïve-like TILs in the tumor-associated stroma. Potential mechanisms for this immune phenotype include a complex network involving the tumor endothelial vasculature and the fibrotic matrix deposited by CAFs and immunosuppressive myeloid cells that restrain TILs in the stroma. Desert OCs are characterized by the total absence of TILs, probably because of the low expression of antigens and immune-activating signals as well as high immune suppression.

The complex cellular crosstalk involved in each OC immune phenotype, and their specific role are only partially understood. Addressing these gaps will be crucial for developing effective therapeutic strategies and maximizing the clinical outcome of patients with OC (see Outstanding questions).

Spatial and temporal heterogeneity of cell–cell crosstalk in OC

ITH and TME variations across primary and metastatic intraperitoneal anatomic sites are highly prevalent in OCs [8,17,19,47], which could affect the frequency and composition of cellular crosstalk. For example, in contrast to homologous recombination repair-proficient (HRP) tumors,

the anatomic sites of primary adnexal HRD tumors are found to be enriched in T cell–myeloid cell networks. These sites exhibit the highest levels of antigen-experienced/exhausted TILs and activated myeloid cell states overexpressing the interferon (IFN)-inducible chemokines CXCL9/CXCL10 [23]. By contrast, distant intraperitoneal metastatic sites are impoverished in exhausted T cells and $CXCL10^{+}$ macrophages and are more infiltrated by naïve-like or central memory T cells [15,47], demonstrating that both genetics and anatomy sculpt immune cell partners in OC.

The mechanisms accounting for such variations of tumor T cell–myeloid cell crosstalk include loss of human leukocyte antigen (HLA) expression through deletion of chromosome 6p harboring HLA class I and II genes [47] and epigenetic silencing of the DNA-sensing/IFN pathway and/or loss of tumor-intrinsic chemokines [22]. Thus, the anatomic site itself could impose distinct selective pressures that potentially drive and/or select for specific phenotypic states of malignant cells. Interestingly, distal intraperitoneal anatomic sites of HRP tumors display TGF-β upregulation, a known driver of immune suppression and T cell exclusion [47].

The omentum represents the most common peritoneal metastatic site for OC, probably owing to the unique proangiogenic vasculature present at this site and/or a potent immunosuppressive effect [48]. Cancer cells invading omental anatomic sites can reprogram stromal cells, such as mesothelial cells, adipocytes, CAFs, endothelial cells, and resident immune cells found in so-called milky spots, to support cancer cell survival and metastasis. While milky spots of the omentum can function as unique secondary lymphoid organs that promote immunity to peritoneal antigens [49], it appears that these sites are unable to promote adaptive immune responses during OC metastasis. One potential mechanism that correlated with suppression of T cell function and poor prognosis in patients with OC is the VEGF-driven accumulation of $CD33^{+}$ MDSCs in the omentum [48].

In addition, omental TME reprogramming was previously characterized by upregulation of collagen-remodeling genes (*COL11A1*, *COMP*, *VCAN*, *FN1*, *COL1A1*, and *CTSB*) that predicted poor survival in patients with OC [38]. Emerging cellular interactions that facilitate tumor invasion were identified between platelets and mesothelial cells. Platelets activate the mesothelium by stimulating ECM and epithelial-to-mesenchymal transition (EMT) processes in mesothelial cells and promote tumor invasion. This could explain why platelets are associated with a poor-prognosis tissue composition in culture models [50].

Standard-of-care therapy (i.e., chemotherapy, PARP inhibitors, etc.), along with tumor evolution, can profoundly remodel the OC TMEs coexisting within a patient [51]. The spatiotemporal evolution of the TME has been described in the context of neoadjuvant chemotherapy [18]. Ligand–receptor analysis identified the TIGIT-NECTIN2 T cell–myeloid cell interaction as a potential target to prevent $CD8^{+}$ T cell exhaustion in response to chemotherapy in OC. More recently, the immunobiology and evolution of OC were dissected by studying paired primary and recurrent tumor samples through digital pathology analysis [20]. TILs and myeloid cell networks were again identified as being central to the immunobiology of OC and were associated with tumor evolution following chemotherapy. Specifically, inflamed tumors exhibited high T cell–DC interactions, whereas recurrent cold tumors were characterized by the accumulation of immunosuppressive myeloid interactions, particularly involving *TREM2*/$APOE^{high}$ TAMs, further supporting the notion that OC progression is regulated by phenotypic changes in DCs and macrophages induced at least in part by tumor cell-derived PGE2, TGF-β1, and ATX/LPA2 [52].

Finally, and despite intrapatient variability, immune escape appears to be a common theme in end-stage disease [53]. A broad reduction in several immune cell subsets was observed in end-stage OC, resulting in a dramatic prevalence of immunologically cold tumors. *CCL5*

hypermethylation and HLA loss of heterozygosity were the most major contributors to diminished TIL recruitment and retention in end-stage OC [53].

It is therefore evident that, to guide new therapeutic opportunities, multisite tumor profiling together with a deep investigation of immune evolution patterns during treatment and recurrence would bring insights into how cellular interactions within the OC TME evolve. This can inform clinical decisions for precision OC therapy.

Computational and imaging approaches to predict and map cell–cell interaction networks in the TME

Tissue staining with hematoxylin and eosin (H&E) and immunohistochemistry (IHC) provide spatial, morphological, and protein expression data which are to some extent sufficient to establish diagnosis and prognosis for OC patients. For example, larger microstructures within the TME such as TLSs can readily be identified by H&E staining. However, multiplexed tissues imaging is necessary to identify heterogeneous cell states and unravel their spatial arrangements in the broader TME landscape.

Single cell-resolution technologies, such as multiplex tissue imaging, hold this potential (Box 1). Multiplex imaging platforms share common analytical pipelines and have defined output datasets which include cell-specific phenotype and position *(x and y* coordinates) across a tissue. This

Box 1. Spatial distribution and protein expression assessment

Recent advances in multiplex tissue imaging technologies have expanded the range of markers and areas analyzed, including tissue microarrays (TMAs) and whole-tissue slides. Spectral deconvolution techniques typically accommodate four to eight markers per cycle of multiplex immunofluorescence (mIF) imaging. mIF can be achieved using conjugated fluorophores [tissue-based cyclic immunofluorescence (t-CyCIF), COMET™, and iterative bleaching extends multiplexity (IBEX) platforms], chromogenic amplification (Opal-immunohistochemistry, IHC) or metal-based antibody detection [multiplexed ion beam imaging (MIBI) by time of flight (TOF), and imaging mass cytometry (IMC)] that support higher multiplexing through iterative staining cycles.

Opal-IHC allows the simultaneous measurement of up to eight markers, enabling the identification and quantification of various cell populations at the protein level in the TME. It utilizes tyramide signal amplification (TSA), where tyramide can be biotinylated or labeled with a fluorescent dye catalyzed by streptavidin–horseradish peroxidase (HRP). The technology uses multiple lasers and specific optics for spectral detection. Digital spectral 'unmixing' corrects for fluorescence emission overlaps, ensuring accurate detection. The Opal workflow uses a stripping protocol to remove primary and secondary HRP-conjugated antibodies, allowing serial IHC despite the complexity of potential epitope damage and signal loss during sequential staining [77].

t-CyCIF uses iterative staining, imaging, and chemical quenching cycles with fluorophore-conjugated antibodies and enables detailed spatial mapping of protein expression and interactions by detecting >60 different proteins in formalin-fixed, paraffin-embedded (FFPE) samples. This technology relies on standard reagents and instruments, making it easy to implement in research laboratories, although it faces signal-to-noise ratio challenges with low protein levels and increased cycle numbers [78]. Incorporating a fully automated microfluidic device into the staining process minimizes staining volumes and wash reagents, and preserves tissue and epitope integrity while increasing homogenous staining. With the ability to stain up to 40 markers within 1 day, incorporating this technology offers a valuable high-throughput approach for TME characterization and advancing cancer research [79].

To further reduce autofluorescence and signal overlap, new methods such as IMC and MIBI have been developed. IMC and MIBI-TOF are advanced IHC technologies for analyzing cell subtypes, interactions, and protein quantities at the subcellular level. IMC uses heavy metal isotopes and laser ablation to provide spatial information and highlight tumor heterogeneity, and can capture >40 protein markers simultaneously on tissue sections with subcellular resolution. Although IMC eliminates autofluorescence, it lacks signal amplification and has slow image acquisition.

Similarly, MIBI-TOF uses a secondary ion mass spectrometer to image antibodies tagged with isotopically heavy metal reporters. Samples are incubated with lanthanide-conjugated primary antibodies, then ionized with a duoplasmatron primary ion beam (i.e., O_2^+ and Xe^+), resulting in lanthanide adducts of the bound antibodies as secondary ions that can be measured by TOF. MIBI can analyze up to 100 targets simultaneously in single cells with spatial resolution [80]. This method can also be combined with single-cell metabolic regulome profiling (scMEP) to predict cancer outcomes and therapeutic effects. Although MIBI offers high specificity and the ability to capture many targets, it is time-consuming and it uses expensive metals [81].

enables digital reconstruction of the cell architecture of tissues and the interrogation of cellular interactions and cellular neighborhoods within them.

Although the development of novel high-plex mIF technologies has facilitated the discovery of crucial cellular interactions such as TIL–myeloid cell interactions for antitumor immune responses in OC, it is important to note that only targets for which suitable antibodies have been developed and validated can be explored. In addition, prior knowledge is necessary to curate an informative selection of probe targets for investigation, thereby limiting the likelihood of uncovering entirely novel types of molecular crosstalk. To further deepen our comprehension of complex cellular interactions, technologies that integrate spatial information with high-throughput molecular analyses are required. Single-cell RNA sequencing (scRNA-seq) has been instrumental in characterizing the cellular composition of the TME in OC [11,47] (Box 2). While scRNA-seq data do not directly capture cellular interactions, the gene expression information of every cell enables the inference and quantification of these networks by incorporating ligand–receptor pair expression and downstream target activation from curated databases (Box 2). However, because scRNA-seq requires single-cell dissociation, the dataset involves loss of spatial distribution and organization. Therefore, tissue validation of inferred interactions by mIF tissue imaging or spatial transcriptomics (Box 3) is necessary.

Rapid advances in spatial transcriptomics have provided insights into the spatial dimension governing cellular crosstalk, allowing researchers to dissect the spatial heterogeneity of the OC TME [43,54–56] (Box 3) and providing an unprecedented opportunity to unravel cellular interactions. Spatial transcriptomics – at a resolution of 20–50 cells – combined with mIF was used to characterize both intra- and interstromal heterogeneity in treatment-naïve advanced-stage OC

Box 2. Single-cell RNA sequencing (scRNA-seq) for inference of cell–cell crosstalk

scRNA-seq has paved the way for deeper investigations of cell–cell crosstalk. By leveraging curated databases covering prior knowledge of intercellular interactions and ligand–receptor pairs, various computational tools have emerged which aim to infer cellular interactions [82]. These tools can be broadly categorized into two main approaches. The first group relies on intercellular events and primarily uses the gene expression of ligand–receptor pairs and their subunits. Core tools such as InterCellDB, SingleCellSignalR, and CCInx, as well as multimeric subunit tools which include mediators of interactions, such as CellChat, ICELLNET, and CellPhoneDB, enhance cell–cell crosstalk analysis by considering complex ligand–receptor interactions (LRIs) [83]. However, gene coexpression is not always indicative of protein interaction.

To address this, in addition to gene expression of ligands, receptors, and their direct regulatory subunits, the second group of tools incorporates prior knowledge of intracellular signaling and gene regulatory networks. Tools such as NicheNet [84], CytoTalk [85], SoptSC [86], scSeqComm [87], and scMLnet [88] allow more comprehensive and biologically relevant predictions of LRIs [89]. Owing to the lack of a gold standard for evaluating LRIs in scRNA-seq, agglomerative tools such as LIANA (ligand–receptor analysis framework) integrate multiple methodologies and resources to produce a consensus for the predicted cell–cell interactions by prioritizing concordant results among the different approaches [82].

A common limitation in the design of cell–cell interaction tools is their restriction to pairwise comparisons [90]. As larger clinical cancer datasets become available, there is a growing need for tools that can handle multiple comparisons across conditions, timepoints, or disease stages, while accounting for covariates and batch effects. Tensor-cell2cell and MultiNicheNet have been developed to address this need [90,91].

Despite the single-cell resolution of scRNA-seq, most tools infer cell–cell interaction between clusters of cells by pseudobulking. This approach aims to mitigate the sparsity inherent to scRNA-seq, gain statistical power, and highlight biological relevant cell–cell interactions at the population level while reducing the computational resources. However, a few tools, such as SpotSC, Niches, Scriabin [92], SPRUCE, and DeepCOLOR, offer the computation of LRIs for individual cells [83].

scRNA-seq loses spatial information, such as the distribution and organization of cells, due to the inherent sample processing procedure. This hinders the understanding of the complex biological relationship and interactions between cells [18,57]. Some tools attempt to overcome this limitation by recreating spatial localization based on assumptions of physical cell interactions. For example, CSOmap [93] and SPROUT [94] use affinity scores between cells based on their LRIs to project them in a pseudo-physical space.

Box 3. Spatial transcriptomics

Spatial transcriptomics enables the investigation of cell–cell crosstalk by preserving spatial context in tissue samples. Two major approaches to spatial transcriptomics have been commercialized, each with distinct strengths and limitations: imaging-based spatial transcriptomics (imST) and sequencing-based spatial transcriptomics (seqST).

ImST technologies visualize gene expression directly in tissue samples by relying on *in situ* hybridization with fluorescent probes. Sequential rounds of hybridization and imaging enable construction of the spatial molecular profile of a tissue [95]. ImST platforms, such as MERSCOPE, 10X Xenium, and CosMx Spatial Molecular Imager, combine single-cell resolution with high RNA capture efficiency [95]. This facilitates detailed spatial mapping of the morphological and cellular heterogeneity of the TME and investigation of immune networks at the molecular and tissue levels [43]. Cell segmentation is a required processing step in imST which delineates cells based on stained morphological features and can be assisted by additional co-stains [96]. Variation in cell boundary identification will alter gene expression and influence downstream analysis [97]. Current imST platforms are limited to capturing hundreds to 1000 unique gene transcripts, and multiplexing samples is technically challenging and resource-intensive.

By contrast, seqST platforms such as Visium and Visium HD from 10X Genomics return high-throughput whole-transcriptomic data by capturing RNA with barcoded arrays and offer unbiased quantification of RNA transcripts. However, seqST technologies provide lower spatial resolution compared to imST, resulting in mixed signals coming from the accumulation of multiple cells. The number of cells captured per single spot can vary greatly depending on the tissue type. Continued increase in the resolution of seqST will alleviate problems associated with agglomeration of cells but will also introduce the need for accurate cell delineation.

New and existing tools have established workflows to accommodate spatial transcriptomics and infer cell–cell interactions with spatially contextualized cells. Tools such as SpaOTsc allow scRNA-seq to be integrated with spatial transcriptomic data and rely on optimal transport to reconstruct the spatial cellular dynamics of the tissue [98]. Giotto, Squidpy, and Cell2Cell are tools that facilitate the analysis of spatial transcriptomic data, and provide information on cellular interactions by identifying spatially resolved cell cluster pairs and their most significant ligand–receptor interactions (LRIs) [83,99]. SpaCET analyzes LRIs within spatial transcriptomic spots to provide evidence of cellular interactions with spatially colocalized cells [100]. Another approach, used in SpatialDM and SpaTalk, is to detect LRIs based on spatial proximity and ligand–receptor coexpression [101]. This can highlight the important role of regional cell–cell interactions in the tissue which can be independent of the cell type or cluster [102]. SpaTalk constrains the possible LRIs spatially to the *k*-nearest neighbors and uses that information to build a cell graph network [102].

samples of patients with either short or extended survival. This study revealed a higher density of proliferating and metabolically active CAFs in stromal clusters from short-term OC survivors (STSs) than in stromal clusters from long term-survivors (LTSs). In addition to typical CAF markers such as α-SMA, VIM, and PDGFRβ, CAFs of STSs overexpressed periostin and CD36 in spatially resolved stromal clusters. Comparative network analysis between STS and LTS samples captured by spatial transcriptomics uncovered crucial interactions between *LRP5*$^{+}$ tumor cells and *APOE*$^{+}$ CAFs located at the tumor–stroma interface [57]. This study is in line with previous reports indicating that an increased matrisome index correlates with poor prognosis [38]. New spatial transcriptomic research that seeks to resolve spatial cellular crosstalk may reveal previously unidentified networks that control tumor immune phenotypes in OC [43].

Modeling and perturbation of cell–cell crosstalk in the TME: systems of *ex vivo* 3D tumor models

The need to understand better how cellular interactions within the TME can influence therapeutic outcomes calls for the development of *ex vivo* model systems that faithfully recapitulate the OC TME and accurately reproduce cellular interactions. Cell culture using 3D models, such as organoids, has been extensively documented in recent years, marking a significant advance in oncology research [58] (Box 4). These *in vitro* models rely on the self-renewal and self-organization of growing cell aggregates derived from pluripotent stem cells that can differentiate under specific conditions involving proteins such as growth factors or small molecules that activate or inhibit particular signaling pathways (Box 4). Organoids can mimic the structural, functional, and biological complexity of an organ [59]. Similarly, patient-derived tumoroids (PDTs), which can be derived directly from harvested OC tissues and ascites, and cultured on different

Box 4. *Ex vivo* model to dissect crosstalk upon perturbation

Organoids are miniaturized, self-organized 3D *in vitro* models of human organs that are derived from healthy tissue-resident adult stem cells, pluripotent stem cells, and/or differentiated cells. Similarly, tumor-like organoids and patient-derived tumoroids (PDTs) can be derived from resected tissue from primary or metastatic tumors. In both models, tissue is dissociated and the cell suspension is embedded in basement membrane extract within a dome or flat matrix such as Matrigel. Alternatively, PDTs can be propagated in plates with microengineered hydrogel-based wells which promote fast and homogenous aggregation of epithelial cells into 3D structures [103]. All models are then overlain with specialized media containing growth factors necessary for deriving and sustaining tumoroids development such as WNT3A, R-spondin, EGF, FGF, noggin, Rock inhibitors, p38 inhibitors, 17β estradiol, and hydrocortisone [58]. Growth factors and media components are tailored based on the origin of the organ from where the tissues are harvested.

Once propagated, PDTs can be maintained by long-term culture (up to 250 days in culture) [104] or cryopreservation. They can faithfully recapitulate the morphological heterogeneity and genetic features of tumor tissue samples from patients [105,106]. Comprising various cell clonotypes from the original tumor, tumoroids can be expanded *in vitro* and allow high-throughput drug screening and biomarker identification. In OC, these models have shown great potential in predicting response and resistance to chemotherapy and PARP inhibitors [64].

Long-term propagated tumoroid cultures are comprised of epithelial cells and are devoid of intrinsic TME components, such as cancer-associated fibroblasts (CAFs), endothelial cells, pericytes, and immune cells. To mimic the cancer niche and the interactions between the tumor and its microenvironment, efforts are underway to reconstruct the TME of PDTs *ex vivo*. This is performed by mixing PDTs with additional stroma cell types such as fibroblasts, adipocytes. mesothelial and endothelial cell as well as immune cells. In addition, PDTs can be used as more faithful models to study the efficacy and infiltration capacity of adoptive cell therapy products *ex vivo*.

Complementary models that incorporate autologous matrix and *in situ* immune components can provide deeper insights into therapy response and resistance mechanisms in OC. These features are offered by PDE, which consists of *ex vivo* culture of freshly resected human tumor slice/fragments. PDE cultures preserve the TME and architecture found in patient tissues. They enable the interrogation of native TME populations and their respective cell–cell crosstalk at baseline or upon perturbation. They can be rapidly generated immediately after surgery and allow evaluation of early response to therapy [71]. However, PDE viability rapidly drops over time, despite optimized culture conditions [73]. One potential reason could be the lack of physiological perfusion of oxygen and nutrients. This limitation can be overcome by implementing perfusion systems and microfluidic devices. These systems can integrate controlled environments with perfusion of soluble growth factors, cytokines, and chemokines, thereby enabling cell–cell interactions, motility, and oxygen perfusion, and improving the long-term viability of 3D models.

scaffolds, can reproduce reliable models of ovarian tumors [60]. PDTs have been shown to maintain the original transcriptomic states and genomic mutations (such as *BRCA1/2*, *TP53*, *KRAS*, and *PIK3CA*) [61], and thus recapitulate the heterogeneous landscape of OC [62]. They have enabled screening studies for PARP inhibitors [63], chemotherapy regimens [61], and epigenetic and targeted therapies [64], and thus are valuable in predicting treatment efficacy for OC [58,61,64,65]. For example, comparative RNA-seq between cisplatin-sensitive and -resistant organoids revealed that fibrillin 1 induces chemoresistance [66]. In addition, upregulation of ECM substrates such as COL6 and increased stiffness mechanisms can elevate resistance to platinum-based chemotherapy in OC organoids [67]. While PDTs may accurately represent the tumor compartment, they lack the stroma and immune compartments of the TME which are essential for tumor cell growth, migration, and invasion in OC (Box 4).

Recent studies have explored the reconstitution of PDTs with various immune components and investigated cellular interactions in coculture settings [68] (Box 4). Tri- and tetra-cultures in 3D, where mesothelial cells, fibroblasts, and adipocytes are isolated from the omentum of the patient and cocultured with tumor cells in an adipocyte-based matrix, showed potential to generate a long-term viable and relevant multicellular model in a semi-high-throughput manner [50]. Furthermore, a PDT coculture with autologous peripheral blood lymphocytes was created to evaluate the efficacy of tumor-reactive T cells [69]. By coculturing OC spheroids and TAMs, it was shown that tumor–TAM interactions promote the progression of OC [70]. In a more holistic approach, anti-PD1/PD-L1 antibodies in IL-2-enriched tumor organoids of OC can sustain endogenous immune cells for 96 h of coculture [65].

Alternatively, patient-derived explants (PDEs) could offer a more faithful representation of the TME and its immune components. PDEs are small, freshly resected human tumor fragments or slices cultured under specific conditions [71,72]. They recapitulate the structural integrity and genetic/phenotypic heterogeneity of the original tumor TME, and enable the study of ITH and cellular crosstalk within the tumor stromal matrix pre- and/or post-perturbation, including chemo/immunotherapy, radiotherapy, and targeted therapies [73,74] (Box 4 and Figure 2). Fluorescence-based and live multiplex imaging of PDEs can also enable visualization of the abundance of cellular interactions *in situ.* For example, time-lapse imaging *ex vivo*, in human and mouse HGSOC tumor tissue slices, was used to measure the motility of $CD8^+$ T and myeloid cells at steady-state and upon perturbation. This study showed that, while *ex vivo* lipopolysaccharide stimulation (which alters macrophage polarization) increased the motility of myeloid cells and T cells, chemotherapy treatment decreased the movement of both $CD8^+$ T and myeloid cells in HGSOC tissue slices [72]. Additional perturbations targeting the PD-1/PD-L1 axis or TIGIT-NECTIN2 ligand–receptor interactions (LRIs) showed the feasibility of using 3D PDE models *ex vivo* to reinvigorate pre-existing tumor-reactive TILs in the TME of OC or melanoma [18,71].

Integrating cutting-edge microfluidic devices with microchip technology introduces a biomechanical dimension while preserving the TME [75]. A recent study reported the feasibility of culturing OC PDEs in agitation-based culture systems for at least 1 month [73]. These OC PDE cultures preserved the histopathological features of the original tumors, with maintenance of the epithelial and stromal components as well as the immune infiltrate. As a proof of concept for the applicability of the model for repeated-dose drug assays, OC PDE cultures were challenged weekly with standard-of-care chemotherapy. An additional study employed these systems to investigate cancer progression mechanisms and immune cell interactions within 3D gel matrices [75]. This approach replicates key structural and functional characteristics of TME *in vivo*, including vasculature (angiogenesis, extravasation), shear stress, nutrient perfusion, blood flow dynamics, and drug distribution, and require small amounts of tissue [76]. To summarize, *ex vivo* model systems, such as PDEs, which can accurately represent the OC TME, can be employed to perturb cell–cell crosstalk and activate antitumor immune responses with different therapeutic approaches.

A working model for mapping and perturbing cellular crosstalk in distinct immune phenotypes of the TME of OC

The findings discussed earlier highlight that understanding and interfering with specific cell–cell crosstalk within predefined OC immune phenotypes holds the potential to predict responses to ICB therapy in patients with OC and further personalize (immune)therapy strategies (Figure 2). In Figure 2 we propose a working model for mapping and perturbing cellular crosstalk in distinct immune phenotypes of the OC TME for the discovery of tissue biomarkers and new actionable targets for OC therapy. First, by employing IHC and mIF, resected tumor tissues (Figure 2Ai) are categorized into $CD8^+$ T cell immune categories (Figure 2Aii). Second, we suggest applying single-cell resolution transcriptomics and proteomics to dissect ligand–receptor pairs (Figure 2Bi) and cell neighborhoods (Figure 2Bii). Third, the inferred baseline cellular crosstalk in *ex vivo* 3D models (Figure 2Ci) can be validated according to the cell networks that are dominant in each specific immune phenotype and perturbed (Figure 2Cii) using different strategies including chemotherapy, targeted therapy, or radiotherapy combined with immunotherapy to reprogram the TME and mobilize both innate and adaptive cells. PDE and PDT models also allow the application and testing of the efficacy of **adoptive cell transfer (ACT)** products such as TILs and chimeric antigen receptor (CAR) or T cell receptor (TCR) T

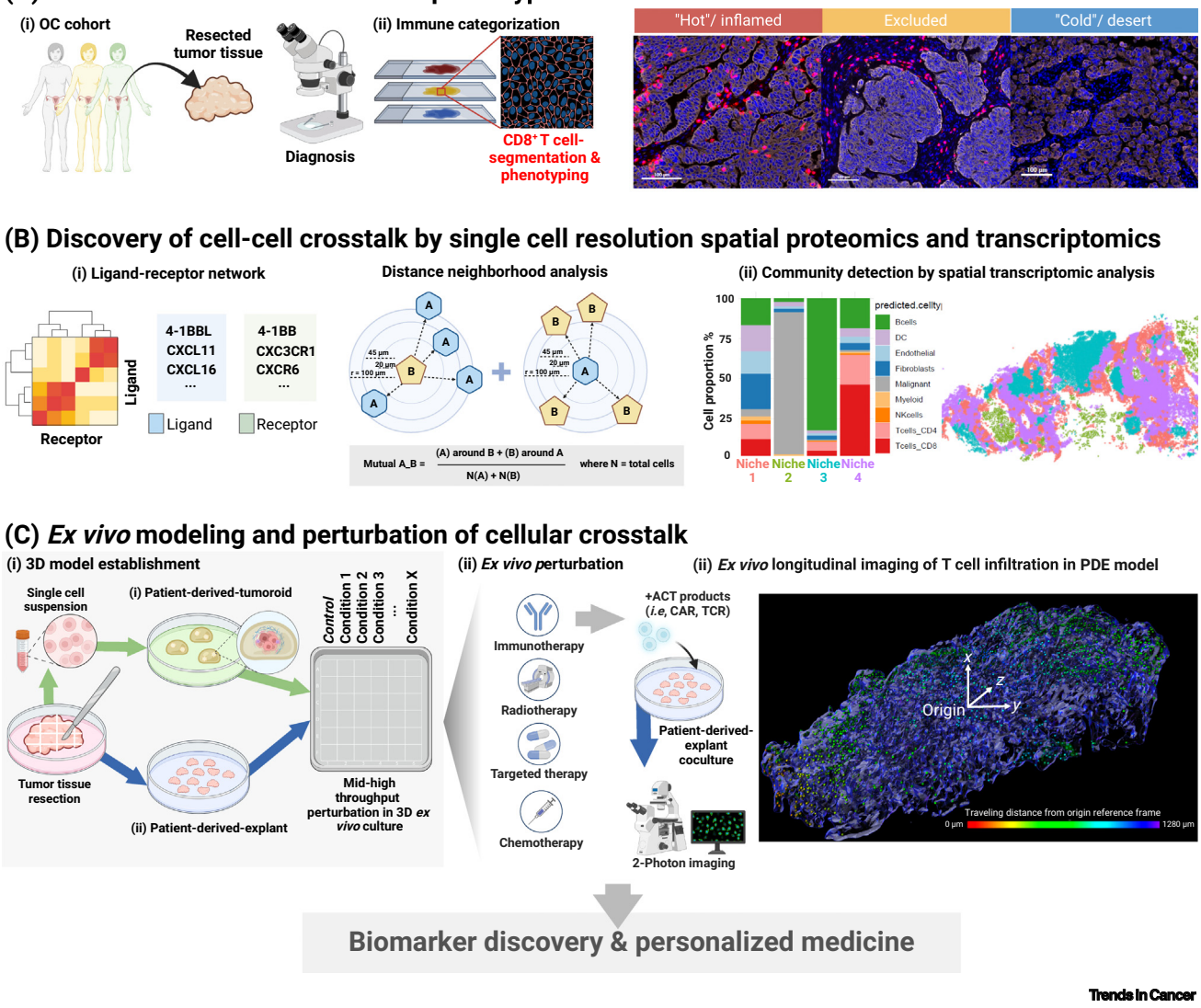

Figure 2. Modeling and perturbation of cell–cell crosstalk of distinct immune phenotypes by using *ex vivo* 3D tumor microenvironment (TME) models. Proposed workflow for mapping and perturbing cellular crosstalk in TME of ovarian cancer (OC) to discover tissue biomarkers and new actionable targets for OC therapy. (Ai) Resected tumor tissues first undergo histopathological evaluation followed by multiplex immunofluorescence (mIF) for $CD8^+$ T cell immune categorization into 'hot'/inflamed, excluded, or 'cold'/desert tumors (Aii). (B) Multi-omic approaches enable profiling of ligand–receptor pairs (Bi) and the cell neighborhood (Bii). (C) Baseline inferred cellular crosstalk can be validated in *ex vivo* PDT and PDE 3D models (Ci), by *ex vivo* perturbation (Cii), and by longitudinal imaging by two-photon microscopy (Ciii) to visualize T cell infiltration in 3D *ex vivo* models (PDE plus ACT coculture). Panel (Bii) is adapted, with permission, from [27]. Abbreviations: ACT, adoptive cell transfer; CAR, chimeric antigen receptor; DC, dendritic cell; miF, multiplex immunofluorescence; NK cell, natural killer cell; PDE, patient-derived explant; PDT, patient-derived tumoroid; TCR, T cell receptor. Figure generated with BioRender.

cell therapies. Visualization of exogenously added TILs in 3D *ex vivo* models can be studied by two-photon imaging (Figure 2Ciii).

This strategy enables the discovery and mid-throughput testing of perturbations that can convert T cell excluded phenotypes into an inflamed phenotype or improve tumor reactivity in already 'hot' tumors (Figure 1). For example, in inflamed tissues, disruption of the PD-1/PD-L1 axis can overcome T cell exhaustion and enhance antitumor activity and upregulate effector functions. In

'excluded' tumors, targeting the PGE2/EP2/EP4 axis and normalizing blood vessels can potentially promote T cell infiltration in tumor islet. Finally, for 'cold' tumors, one can target ECM stiffness by inhibiting the TGF-β/TGF-βR axis in conjunction with ACT therapies (i.e., CAR/TCR T cells).

Concluding remarks

As we have comprehensively reported in this review, T cell infiltration and functionality within the TME are tightly regulated by cell–cell and molecular crosstalk. Immune phenotypic classification of OCs based on $CD8^+$ T cell distribution provides a strong basis to improve our understanding of the molecular and cellular determinants of T cell infiltration. For example, intratumoral TIL–myeloid interactions as well as B cell-dominated TLS structures represent hallmarks of an antitumor immune response in inflamed OC immune phenotypes. By contrast, $CD8^+$ T cell immune networks of excluded and desert immune phenotypes are severely impeded by immunosuppressive myeloid cells together with a strong stromal barrier enabled by the vasculature and CAFs as well as their respective ECM.

We propose that this framework can reveal key types of cell–cell crosstalk that characterize the different immune phenotypes of the OC TME and can be employed as tissue biomarkers to select patients for (immune)therapy (see Outstanding questions). Single-cell resolution technologies such as multiplex tissue imaging and spatial transcriptomics hold the potential to identify heterogeneous TME cell states and unravel their spatial organization. Looking to the future, the integration of detailed TME studies with *ex vivo* perturbation 3D models will lead to the discovery of new and intricate cellular interactions within the TME, thereby offering insights into the biological mechanisms of immune resistance and pointing towards novel therapeutic strategies for the treatment of OC (see Outstanding questions).

Outstanding questions

Are the endogenous immunity and tumor immune phenotypes in OC maintained during treatment and tumor evolution?

What are the cellular crosstalk and molecular networks which regulate TLS neogenesis and establishment in OC? How does treatment affect TLSs?

What is the role of $CD4^+$ T subsets and other cell types such as neutrophils, innate lymphoid cells, mast cells, and platelets in the immunobiology of OC?

How are myelopoiesis and the recruitment of myeloid progenitors regulated in OC? What are the factors that force the polarization of myeloid cells into immunosuppressive states?

How do the ECM and stroma of excluded/desert tumors regulate the differentiation and expansion of infiltrating tumor-reactive TILs? Does the ECM actively prevent tumor-reactive TILs from infiltrating the tumor bed, or does it retain them in a naïve state?

How could we target the stroma ECM to make it permissive for TIL infiltration?

Can we expect multiplexed imaging techniques to be applied to clinical diagnostics and inform therapeutic decisions?

How can the generation of PDEs be standardized and streamlined to be clinically applicable in OC research?

Author contributions

D.D.L., B.S.C., N.R., A.J.G., and E.G. researched data and wrote this article. D.D.L. conceived the article, provided supervision, and made substantial contributions to the discussion of the content. D.D.L., E.G., and B.S.C. revised and finalized article submission. All authors reviewed and/or edited the manuscript before submission.

Acknowledgments

This work was supported by the Ludwig Institute for Cancer Research and a Department of Defense (DOD) Early Career Investigator (ECI) W81XWH2210703 award OC210038 to D.D.L. Any views, opinions, findings, conclusions, or recommendations expressed in this material are those solely of the authors and not necessarily reflect those of DOD.

Declaration of interests

D.D.L. has received funding from Hoffmann-La Roche AG. The remaining authors declare no competing interests.

References

1. Colombo, N. *et al.* (2021) Pembrolizumab for persistent, recurrent, or metastatic cervical cancer. *N. Engl. J. Med.* 385, 1856–1867
2. Makker, V. *et al.* (2022) Lenvatinib plus pembrolizumab for advanced endometrial cancer. *N. Engl. J. Med.* 386, 437–448
3. Kandalaft, L.E. *et al.* (2022) Immunobiology of high-grade serous ovarian cancer: lessons for clinical translation. *Nat. Rev. Cancer* 22, 640–656
4. Ghisoni, E. *et al.* (2019) Ovarian cancer immunotherapy: turning up the heat. *Int. J. Mol. Sci.* 20, 2927
5. Zhang, L. *et al.* (2003) Intratumoral T cells, recurrence, and survival in epithelial ovarian cancer. *N. Engl. J. Med.* 348, 203–213
6. Hao, J. *et al.* (2020) Prognostic impact of tumor-infiltrating lymphocytes in high grade serous ovarian cancer: a systematic review and meta-analysis. *Ther. Adv. Med. Oncol.* 12, 1758835920967241
7. Sato, E. *et al.* (2005) Intraepithelial $CD8^+$ tumor-infiltrating lymphocytes and a high $CD8^+$/regulatory T cell ratio are associated with favorable prognosis in ovarian cancer. *Proc. Natl. Acad. Sci. USA* 102, 18538–18543
8. Dangaj Laniti, D. and Coukos, G. (2022) Genetics and anatomy sculpt immune-cell partners of ovarian cancer. *Nature* 612, 634–636
9. Landen, C.N. *et al.* (2023) Influence of genomic landscape on cancer immunotherapy for newly diagnosed ovarian cancer: biomarker analyses from the IMagyn050 randomized clinical trial. *Clin. Cancer Res.* 29, 1698–1707
10. Anadon, C.M. *et al.* (2022) Ovarian cancer immunogenicity is governed by a narrow subset of progenitor tissue-resident memory T cells. *Cancer Cell* 40, 545–557
11. Hornburg, M. *et al.* (2021) Single-cell dissection of cellular components and interactions shaping the tumor immune phenotypes in ovarian cancer. *Cancer Cell* 39, 928–944
12. Duraiswamy, J. *et al.* (2021) Myeloid antigen-presenting cell niches sustain antitumor T cells and license PD-1 blockade via CD28 costimulation. *Cancer Cell* 39, 1623–1642
13. Fridman, W.H. *et al.* (2017) The immune contexture in cancer prognosis and treatment. *Nat. Rev. Clin. Oncol.* 14, 717–734

14. Ovarian Tumor Tissue Analysis (OTTA) Consortium *et al.* (2017) Dose–response association of CD8$^+$ tumor-infiltrating lymphocytes and survival time in high-grade serous ovarian cancer. *JAMA Oncol.* 3, e173290
15. Garsed, D.W. *et al.* (2022) The genomic and immune landscape of long-term survivors of high-grade serous ovarian cancer. *Nat. Genet.* 54, 1853–1864
16. Desbois, M. *et al.* (2020) Integrated digital pathology and transcriptome analysis identifies molecular mediators of T-cell exclusion in ovarian cancer. *Nat. Commun.* 11, 5583
17. Zhang, A.W. *et al.* (2018) Interfaces of malignant and immunologic clonal dynamics in ovarian cancer. *Cell* 173, 1755–1769
18. Launonen, I.M. *et al.* (2024) Chemotherapy induces myeloid-driven spatial T-cell exhaustion in ovarian cancer. *BioRxiv*, Published online March 20, 2024. https://doi.org/10.1101/2024.03.19.585657
19. Jimenez-Sanchez, A. *et al.* (2020) Unraveling tumor-immune heterogeneity in advanced ovarian cancer uncovers immunogenic effect of chemotherapy. *Nat. Genet.* 52, 582–593
20. Ghisoni, E. (2024) Myeloid cell networks determine reinstatement of original immune environments in recurrent ovarian cancer. *BioRxiv*, Published online May 5, 2024. https://doi.org/10.1101/2024.05.02.590528
21. Parkes, E.E. *et al.* (2017) Activation of STING-dependent innate immune signaling by S-phase-specific DNA damage in breast cancer. *J. Natl. Cancer Inst.* 109, dhw199
22. Bruand, M. *et al.* (2021) Cell-autonomous inflammation of BRCA1-deficient ovarian cancers drives both tumor-intrinsic immunoreactivity and immune resistance via STING. *Cell Rep.* 36, 109412
23. Dangaj, D. *et al.* (2019) Cooperation between constitutive and inducible chemokines enables T cell engraftment and immune attack in solid tumors. *Cancer Cell* 35, 885–900
24. Muthuswamy, R. *et al.* (2021) CXCR6 by increasing retention of memory CD8$^+$ T cells in the ovarian tumor microenvironment promotes immunosurveillance and control of ovarian cancer. *J. Immunother. Cancer* 9, e003329
25. Truxova, I. *et al.* (2018) Mature dendritic cells correlate with favorable immune infiltrate and improved prognosis in ovarian carcinoma patients. *J. Immunother. Cancer* 6, 139
26. Ledermann, J.A. *et al.* (2023) Molecular determinants of clinical outcomes of pembrolizumab in recurrent ovarian cancer: exploratory analysis of KEYNOTE-100. *Gynecol. Oncol.* 178, 119–129
27. Barras, D. *et al.* (2024) Response to tumor-infiltrating lymphocyte adoptive therapy is associated with preexisting CD8$^+$ T-myeloid cell networks in melanoma. *Sci. Immunol.* 9, eadg7995
28. Conejo-Garcia, J.R. *et al.* (2023) Neglected no more: B cell-mediated anti-tumor immunity. *Semin. Immunol.* 65, 101707
29. Kasikova, L. *et al.* (2024) Tertiary lymphoid structures and B cells determine clinically relevant T cell phenotypes in ovarian cancer. *Nat. Commun.* 15, 2528
30. Biswas, S. *et al.* (2021) IgA transcytosis and antigen recognition govern ovarian cancer immunity. *Nature* 591, 464–470
31. Mazor, R.D. *et al.* (2022) Tumor-reactive antibodies evolve from non-binding and autoreactive precursors. *Cell* 185, 1208–1222
32. Ukita, M. *et al.* (2022) CXCL13-producing CD4$^+$ T cells accumulate in the early phase of tertiary lymphoid structures in ovarian cancer. *JCI Insight* 7, e157215
33. Sautes-Fridman, C. *et al.* (2019) Tertiary lymphoid structures in the era of cancer immunotherapy. *Nat. Rev. Cancer* 19, 307–325
34. Mondal, T. *et al.* (2023) Characterizing the regulatory Fas (CD95) epitope critical for agonist antibody targeting and CAR-T bystander function in ovarian cancer. *Cell Death Differ.* 30, 2408–2431
35. Morotti, M. *et al.* (2024) PGE2 inhibits TIL expansion by disrupting IL-2 signalling and mitochondrial function. *Nature* 629, 426–434
36. Lacher, S.B. *et al.* (2024) PGE(2) limits effector expansion of tumour-infiltrating stem-like CD8$^+$ T cells. *Nature* 629, 417–425
37. Rahma, O.E. and Hodi, F.S. (2019) The intersection between tumor angiogenesis and immune suppression. *Clin. Cancer Res.* 25, 5449–5457
38. Pearce, O.M.T. *et al.* (2018) Deconstruction of a metastatic tumor microenvironment reveals a common matrix response in human cancers. *Cancer Discov.* 8, 304–319
39. Mariathasan, S. *et al.* (2018) TGFbeta attenuates tumour response to PD-L1 blockade by contributing to exclusion of T cells. *Nature* 554, 544–548
40. Kennel, K.B. *et al.* (2023) Cancer-associated fibroblasts in inflammation and antitumor immunity. *Clin. Cancer Res.* 29, 1009–1016
41. LeBleu, V.S. and Kalluri, R. (2018) A peek into cancer-associated fibroblasts: origins, functions and translational impact. *Dis. Model. Mech.* 11, dmm029447
42. Mayer, S. *et al.* (2023) The tumor microenvironment shows a hierarchy of cell–cell interactions dominated by fibroblasts. *Nat. Commun.* 14, 5810
43. Yeh, C.Y. (2023) Mapping ovarian cancer spatial organization uncovers immune evasion drivers at the genetic, cellular, and tissue level. *BioRxiv*, Published online October 19, 2023. https://www.nature.com/articles/s41590-024-01943-5#citeas
44. Pallotta, M.T. *et al.* (2022) Indoleamine 2,3-dioxygenase 1 (IDO1): an up-to-date overview of an eclectic immunoregulatory enzyme. *FEBS J.* 289, 6099–6118
45. Cubillos-Ruiz, J.R. *et al.* (2015) ER stress sensor XBP1 controls anti-tumor immunity by disrupting dendritic cell homeostasis. *Cell* 161, 1527–1538
46. Chopra, S. *et al.* (2019) IRE1alpha–XBP1 signaling in leukocytes controls prostaglandin biosynthesis and pain. *Science* 365, eaau6499
47. Vazquez-Garcia, I. *et al.* (2022) Ovarian cancer mutational processes drive site-specific immune evasion. *Nature* 612, 778–786
48. Meza-Perez, S. and Randall, T.D. (2017) Immunological functions of the omentum. *Trends Immunol.* 38, 526–536
49. Rangel-Moreno, J. *et al.* (2009) Omental milky spots develop in the absence of lymphoid tissue-inducer cells and support B and T cell responses to peritoneal antigens. *Immunity* 30, 731–743
50. Malacrida, B. *et al.* (2021) A human multi-cellular model shows how platelets drive production of diseased extracellular matrix and tissue invasion. *iScience* 24, 102676
51. Jimenez-Sanchez, A. *et al.* (2017) Heterogeneous tumor-immune microenvironments among differentially growing metastases in an ovarian cancer patient. *Cell* 170, 927–938
52. Chae, C.S. *et al.* (2022) Tumor-derived lysophosphatidic acid blunts protective type I interferon responses in ovarian cancer. *Cancer Discov.* 12, 1904–1921
53. Burdett, N.L. *et al.* (2023) Multiomic analysis of homologous recombination-deficient end-stage high-grade serous ovarian cancer. *Nat. Genet.* 55, 437–450
54. Denisenko, E. *et al.* (2024) Spatial transcriptomics reveals discrete tumour microenvironments and autocrine loops within ovarian cancer subclones. *Nat. Commun.* 15, 2860
55. Stur, E. *et al.* (2022) Spatially resolved transcriptomics of high-grade serous ovarian carcinoma. *iScience* 25, 103923
56. Zhang, L. *et al.* (2024) Single-cell analysis reveals the stromal dynamics and tumor-specific characteristics in the microenvironment of ovarian cancer. *Commun. Biol.* 7, 20
57. Ferri-Borgogno, S. *et al.* (2023) Spatial transcriptomics depict ligand–receptor cross-talk heterogeneity at the tumor-stroma interface in long-term ovarian cancer survivors. *Cancer Res.* 83, 1503–1516
58. Chan, W.S. *et al.* (2023) Patient-derived organoid culture in epithelial ovarian cancers – tyechniques, applications, and future perspectives. *Cancer Med.* 12, 19714–19731
59. Zhao, Z. *et al.* (2022) Organoids. *Nat. Rev. Methods Primers* 2, 94
60. Tatullo, M. *et al.* (2020) Organoids in translational oncology. *J. Clin. Med.* 9, 2774
61. Kopper, O. *et al.* (2019) An organoid platform for ovarian cancer captures intra- and interpatient heterogeneity. *Nat. Med.* 25, 838–849
62. de Witte, C.J. *et al.* (2020) Patient-derived ovarian cancer organoids mimic clinical response and exhibit heterogeneous inter- and intrapatient drug responses. *Cell Rep.* 31, 107762
63. Hill, S.J. *et al.* (2018) Prediction of DNA repair inhibitor response in short-term patient-derived ovarian cancer organoids. *Cancer Discov.* 8, 1404–1421
64. Nanki, Y. *et al.* (2020) Patient-derived ovarian cancer organoids capture the genomic profiles of primary tumours applicable for drug sensitivity and resistance testing. *Sci. Rep.* 10, 12581

65. Wan, C. *et al.* (2021) Enhanced efficacy of simultaneous PD-1 and PD-L1 immune checkpoint blockade in high-grade serous ovarian cancer. *Cancer Res.* 81, 158–173
66. Wang, Z. *et al.* (2022) The fibrillin-1/VEGFR2/STAT2 signaling axis promotes chemoresistance via modulating glycolysis and angiogenesis in ovarian cancer organoids and cells. *Cancer Commun. (Lond.)* 42, 245–265
67. Pietila, E.A. *et al.* (2021) Co-evolution of matrisome and adaptive adhesion dynamics drives ovarian cancer chemoresistance. *Nat. Commun.* 12, 3904
68. Jeong, S.R. and Kang, M. (2023) Exploring tumor–immune interactions in co-culture models of T cells and tumor organoids derived from patients. *Int. J. Mol. Sci.* 24, 14609
69. Dijkstra, K.K. *et al.* (2018) Generation of tumor-reactive T cells by co-culture of peripheral blood lymphocytes and tumor organoids. *Cell* 174, 1586–1598
70. Long, L. *et al.* (2021) Tumor-associated macrophages induced spheroid formation by CCL18–ZEB1–M-CSF feedback loop to promote transcoelomic metastasis of ovarian cancer. *J. Immunother. Cancer* 9, e003973
71. Voabil, P. *et al.* (2021) An ex vivo tumor fragment platform to dissect response to PD-1 blockade in cancer. *Nat. Med.* 27, 1250–1261
72. Laforets, F. *et al.* (2023) Semi-supervised analysis of myeloid and T cell behavior in ex vivo ovarian tumor slices reveals changes in cell motility after treatments. *iScience* 26, 106514
73. Abreu, S. *et al.* (2020) Patient-derived ovarian cancer explants: preserved viability and histopathological features in long-term agitation-based cultures. *Sci. Rep.* 10, 19462
74. Ricciardelli, C. *et al.* (2018) Novel ex vivo ovarian cancer tissue explant assay for prediction of chemosensitivity and response to novel therapeutics. *Cancer Lett.* 421, 51–58
75. Li, Y. *et al.* (2022) Microfluidic devices: the application in TME modeling and the potential in immunotherapy optimization. *Front. Genet.* 13, 969723
76. Dadgar, N. *et al.* (2020) A microfluidic platform for cultivating ovarian cancer spheroids and testing their responses to chemotherapies. *Microsyst. Nanoeng.* 6, 93
77. Eng, J. *et al.* (2022) A framework for multiplex imaging optimization and reproducible analysis. *Commun. Biol.* 5, 438
78. Lin, J.R. *et al.* (2018) Highly multiplexed immunofluorescence imaging of human tissues and tumors using t-CyCIF and conventional optical microscopes. *Elife* 7, e31657
79. Rivest, F. *et al.* (2023) Fully automated sequential immunofluorescence (seqIF) for hyperplex spatial proteomics. *Sci. Rep.* 13, 16994
80. Funingana, I.G. *et al.* (2023) Multiparameter single-cell proteomic technologies give new insights into the biology of ovarian tumors. *Semin. Immunopathol.* 45, 43–59
81. Hartmann, F.J. *et al.* (2021) Single-cell metabolic profiling of human cytotoxic T cells. *Nat. Biotechnol.* 39, 186–197
82. Dimitrov, D. *et al.* (2022) Comparison of methods and resources for cell–cell communication inference from single-cell RNA-Seq data. *Nat. Commun.* 13, 3224
83. Armingol, E. *et al.* (2024) The diversification of methods for studying cell–cell interactions and communication. *Nat. Rev. Genet.* 25, 381–400
84. Browaeys, R. *et al.* (2020) NicheNet: modeling intercellular communication by linking ligands to target genes. *Nat. Methods* 17, 159–162
85. Hu, Y. *et al.* (2021) CytoTalk: de novo construction of signal transduction networks using single-cell transcriptomic data. *Sci. Adv.* 7, eabf1356
86. Wang, S. *et al.* (2019) Cell lineage and communication network inference via optimization for single-cell transcriptomics. *Nucleic Acids Res.* 47, e66
87. Baruzzo, G. *et al.* (2022) Identify, quantify and characterize cellular communication from single-cell RNA sequencing data with scSeqComm. *Bioinformatics* 38, 1920–1929
88. Cheng, J. *et al.* (2021) Inferring microenvironmental regulation of gene expression from single-cell RNA sequencing data using scMLnet with an application to COVID-19. *Brief. Bioinform.* 22, 988–1005
89. Peng, L. *et al.* (2024) CellDialog: a computational framework for Ligand–receptor-mediated cell–cell communication analysis III. *IEEE J. Biomed. Health Inform.* 28, 580–591
90. Browaeys, R. (2023) MultiNicheNet: a flexible framework for differential cell-cell communication analysis from multi-sample multi-condition single-cell transcriptomics data. *BioRxiv*, Published online June 14, 2023. https://doi.org/10.1101/2023.06.13.544751
91. Armingol, E. *et al.* (2022) Context-aware deconvolution of cell-cell communication with Tensor-cell2cell. *Nat. Commun.* 13, 3665
92. Wilk, A.J. *et al.* (2024) Comparative analysis of cell-cell communication at single-cell resolution. *Nat. Biotechnol.* 42, 470–483
93. Ren, X. *et al.* (2020) Reconstruction of cell spatial organization from single-cell RNA sequencing data based on ligand-receptor mediated self-assembly. *Cell Res.* 30, 763–778
94. Wang, J. *et al.* (2022) SPROUT: spectral sparsification helps restore the spatial structure at single-cell resolution. *NAR Genom. Bioinform.* 4, lqac069
95. Wang, Y. *et al.* (2023) Spatial transcriptomics: technologies, applications and experimental considerations. *Genomics* 115, 110671
96. Petukhov, V. *et al.* (2022) Cell segmentation in imaging-based spatial transcriptomics. *Nat. Biotechnol.* 40, 345–354
97. Chen, H. *et al.* (2023) SCS: cell segmentation for high-resolution spatial transcriptomics. *Nat. Methods* 20, 1237–1243
98. Cang, Z. and Nie, Q. (2020) Inferring spatial and signaling relationships between cells from single cell transcriptomic data. *Nat. Commun.* 11, 2084
99. Almet, A.A. *et al.* (2021) The landscape of cell–cell communication through single-cell transcriptomics. *Curr. Opin. Syst. Biol.* 26, 12–23
100. Ru, B. *et al.* (2023) Estimation of cell lineages in tumors from spatial transcriptomics data. *Nat. Commun.* 14, 568
101. Shao, X. *et al.* (2022) Knowledge-graph-based cell–cell communication inference for spatially resolved transcriptomic data with SpaTalk. *Nat. Commun.* 13, 4429
102. Li, Z. *et al.* (2023) SpatialDM for rapid identification of spatially co-expressed ligand–receptor and revealing cell–cell communication patterns. *Nat. Commun.* 14, 3995
103. Brandenberg, N. *et al.* (2020) High-throughput automated organoid culture via stem-cell aggregation in microcavity arrays. *Nat. Biomed. Eng.* 4, 863–874
104. Paul, C.D. (2024) Long-term maintenance of patient-specific characteristics in tumoroids from six cancer indications in a common base culture media system. *BioRxiv*, Published online June 12, 2024. https://doi.org/10.1101/2024.06.10.598331
105. Psilopatis, I. *et al.* (2022) Patient-derived organoids: the beginning of a new era in ovarian cancer disease modeling and drug sensitivity testing. *Biomedicines* 11, 1
106. Hoffmann, K. *et al.* (2020) Stable expansion of high-grade serous ovarian cancer organoids requires a low-Wnt environment. *EMBO J.* 39, e104013